Supplementary Information (ESI)

for

Reversible Solid-Gas Chemical Equilibrium between a 0-Periodic Deformable Molecular Tecton and a 3-Periodic Coordination Architecture

Deng Liu,[+] Mian Li[+] and Dan Li*

Department of Chemistry, Shantou University, Guangdong 515063, P. R. China

E-mail: dli@stu.edu.cn

Table of Contents

[+] M. Li and D. Liu contributed equally to this work.

* Corresponding author. E-mail: dli@stu.edu.cn

Experimental Section

Synthesis of ligand: The 3-(pyridin-4-yl)-5-(pyrizin-2-yl)-1*H*-1,2,4-triazole ligand (**L**) was prepared according to the procedure similar to previous literature (W. R. Browne, C. M. O'Connor, H. P. Hughes, R. Hage, O. Walter, M. Doering, J. F. Gallagher, J. G. Vos, *J. Chem. Soc., Dalton Trans.* 2002, 4048).

Synthesis of 1 and 2: A mixture of CuI (0.0190 g, 0.1mmol) and **L** (0.0223 g, 0.1mmol) in methanol solvent (8mL) was stirred for 5 min in air, and then transferred to and sealed in a 15-mL Teflon-lined reactor. The reactor was heated in an oven at 160 ˚C for 72 h, and then cooled to room temperature at a rate of 5 ˚C·h^{-1}. X-ray quality purple (sometimes brown) columnar crystals of **1** (Yield: 68 %) were obtained, accompanying with sporadic green lamellar crystals of **2** as byproducts.

X-ray Crystallography: Crystal data for **1**: $C_{22}H_{14}CuN_{12}$, rhombohedral, space group *R*-3, *Mr* = 509.99, *a* = *b* = 27.226(6) Å, *c* = 8.981(6) Å, $\alpha = \beta = 90.00$ º, $\gamma = 120.00$ º, *V* = 5765.9(42) Å^3, *Z* = 9, *Dc* = 1.322 g cm^{-3}, μ = 0.886 mm^{-1}, *F*(000) = 2331, *T* = 298(2) K; final R_1 = 0.0628, wR_2 = 0.2009, *GOF* = 1.056 for all data. Crystal data for **2**: $C_{22}H_{16}CuN_{12}O$, monoclinic, space group *C2/c*, *Mr* = 528.01, *a* = 23.792(2) Å, *b* = 6.9517(6) Å, *c* = 12.7747(11) Å, $\alpha = 90.00$ º, $\beta = 92.346(2)$ º, $\gamma = 90.00$ º, *V* = 2111.1(3) Å^3, *Z* = 4, *Dc* = 1.661 g cm^{-3}, μ = 1.082 mm^{-1}, *F*(000) = 1076, *T* = 298(2) K; final R_1 = 0.0412, wR_2 = 0.1037, *GOF* = 1.054 for all data. Data collections were performed on a Bruker Smart Apex CCD diffractometer (MoKα radiation, λ = 0.71073 Å) by using frames of 0.3 oscillation ($2\theta < 56$ º) at *T* = 298(2) K using SMART. The structures were solved by direct methods, and all non hydrogen atoms were subjected to anisotropic refinement by full-matrix least-squares methods on F^2 by using the SHELXTL program (G. M. Sheldrick, *SHELXLT 6.10*, Bruker Analytical Instrumentation, Madison, Wisconsin, USA, **2000**). Multi-scan corrections were applied using SADABS. All non-hydrogen atoms were anisotropically refined. Structure solutions and refinements were performed with the SHELXL-97 package (G. M. Sheldrick, *SHELXS-97 and SHELXL-97*, Göttingen University, Göttingen, Germany, **1997**). Though the structure of **1** contained solvent accessible voids of 375.00 Å^3, there is no large peak in data solution, and the TGA pattern of **1** (Figure S4a in SI) also clearly showed that there was no solvent in the lattice.

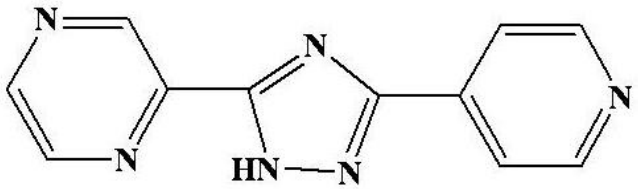

3-(pyridin-4-yl)-5-(pyrizin-2-yl)-1*H*-1,2,4-triazole

Chart S1. Representation of the ligand (**L**).

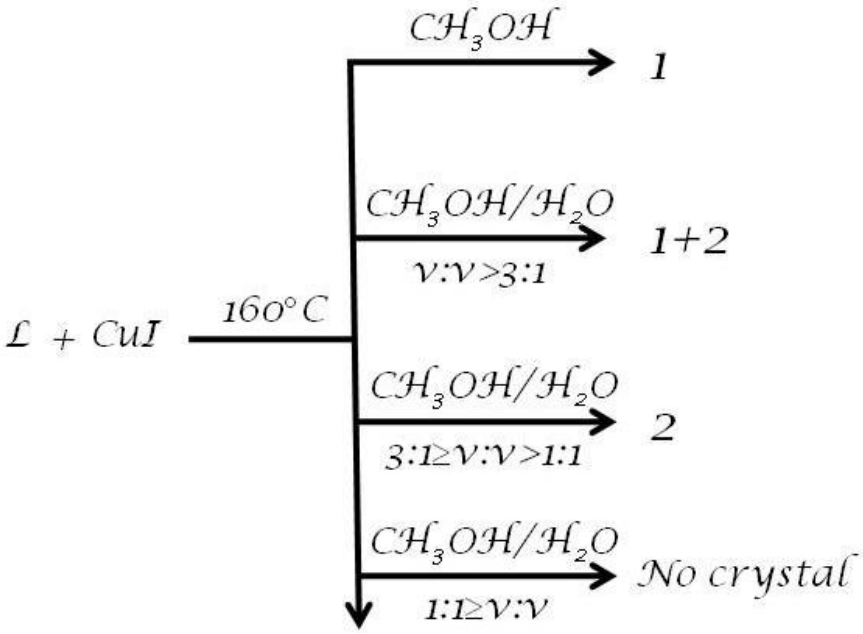

Scheme S1. Control experiments for the synthesis of **1** and **2**.

The byproduct **2** yielded in methanolic solution solvothermally might be due to the trace water existed in methanol, and therefore mixed methanol/water solvents (in sequential rates) were introduced in the control experiments. All other experimental parameters remained constant, except for varying the 8 mL solvent (as shown in Scheme S1). It was reasonable to find that with the augment of water the reaction yield for **2** increased until finally in a certain rate the crystals of **1** vanished, because the water molecules served as competing ligands to manipulate the equilibrium between **1** and **2**. When the content of water exceeded that of methanol (or pure water was used), no single crystal was yielded. This was probably because the solubility of the ligand in the mixed solvents was reduced.

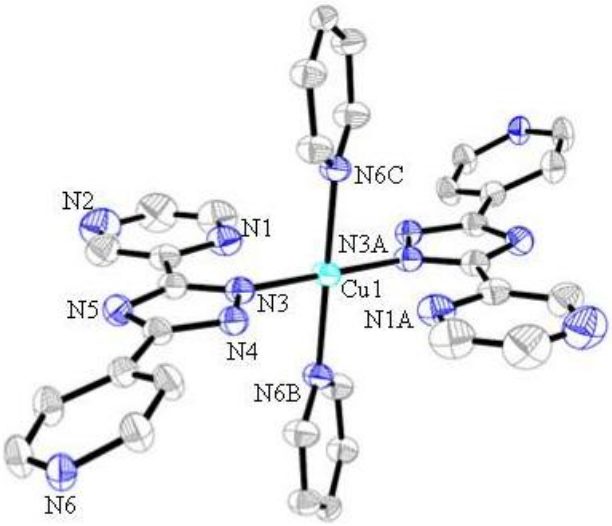

(a)

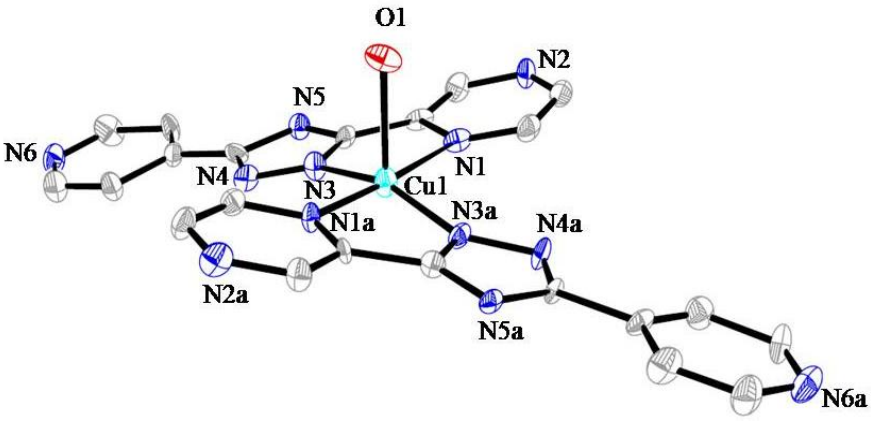

(b)

Figure S1. Coordination environments of copper(II) centers in **1** (a) and **2** (b). All hydrogen atoms are omitted for clarity. Drawn with 30% ellipsoids.

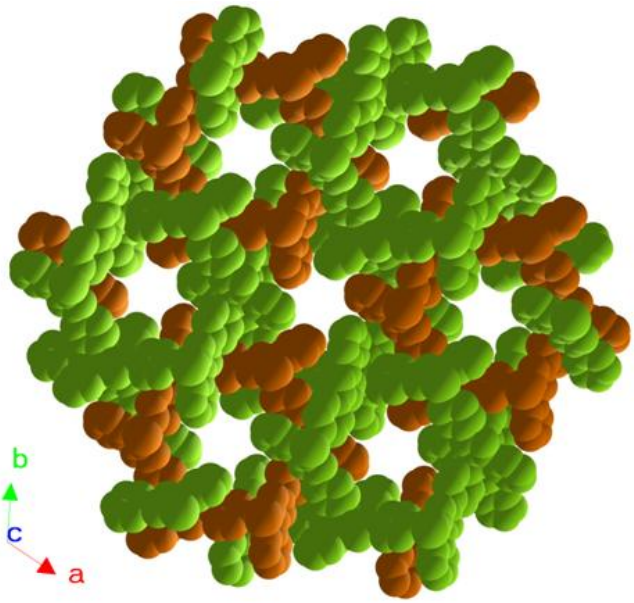

(a)

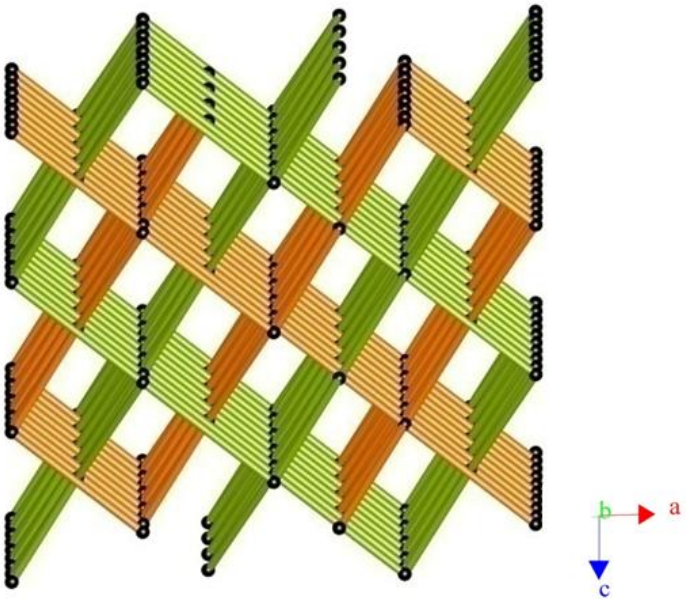

(b)

Figrue S2. Representation of overall structure of **1**. (a) Space filling representation of the 3D two-fold interpenetrating (green and orange) framework, showing the 1D porous channel along the *c* axis. (b) Topological representation of the two-fold interpenetrating (green and orange) NbO-type network, in which each [Cu(**L**)$_2$] tecton is envisioned as a four-connected planar-square node (black). All hydrogen atoms are omitted for clarity.

For details of the NbO net, refer to RCSR: http://rcsr.anu.edu.au/nets/nbo.

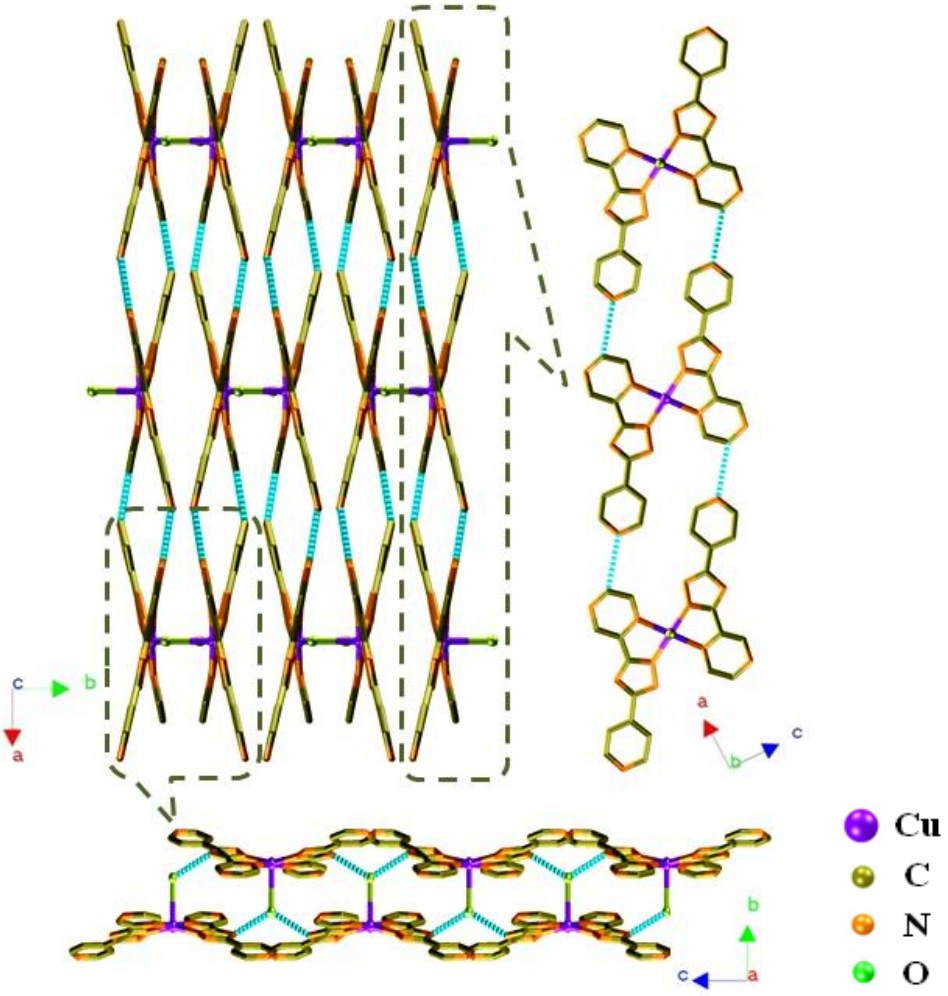

Figrue S3. Representation of overall structure of **2**. The discrete monomer packs densely via intermolecular hydrogen bonding (blue dashed cones). The left top view shows the overall packing. The right top view shows a line of the layer tilling packing parallel to the *ac* plane, in which each pair of tectons are linked via two sets of weak C–H···N hydrogen bondings. The bottom view shows the strong O–H···N hydrogen bondings among adjacent layers. All hydrogen atoms are omitted for clarity.

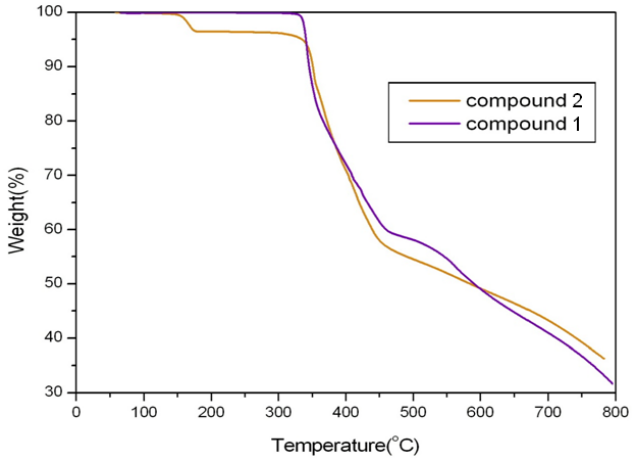

(a)

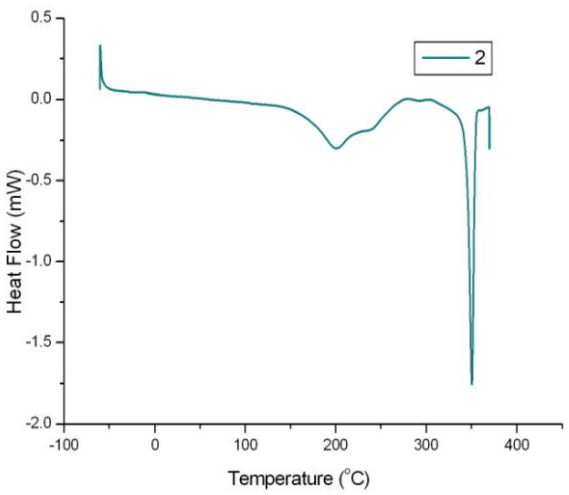

(b)

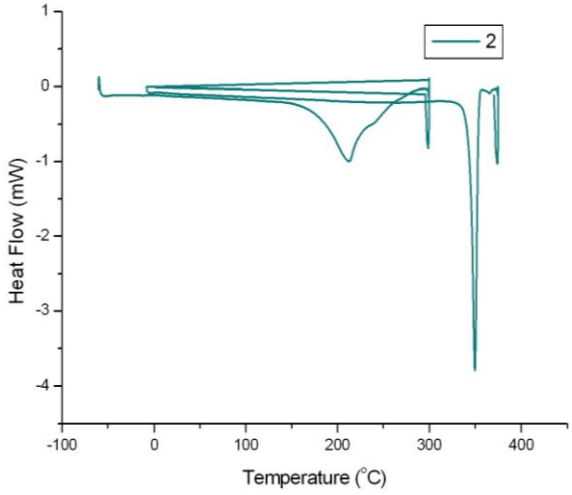

(c)

Figrue S4. TGA and DSC patterns for **2**. (a) TGA patterns. The TGA for **2** displayed a weight loss of approximate 3.6 % at about 160 °C, which could be attributed to the loss of the labile metal-bound water ligands (calculated loss of 3.4 %), and then the residue stayed stable up to 350 °C. (b) DSC pattern. The DSC for **2** showed that the endothermic ΔH value for the dehydration process was about 90 kJ·mol^{-1}. (c) Stepwise DSC pattern: The sample of **2** was heated to undergo the dehydration process and then cooled to room temperature, and then was reheated but showed no endothermic peak in the dehydration region. This indicated that the residue maintained a stable phase (probably **1**).

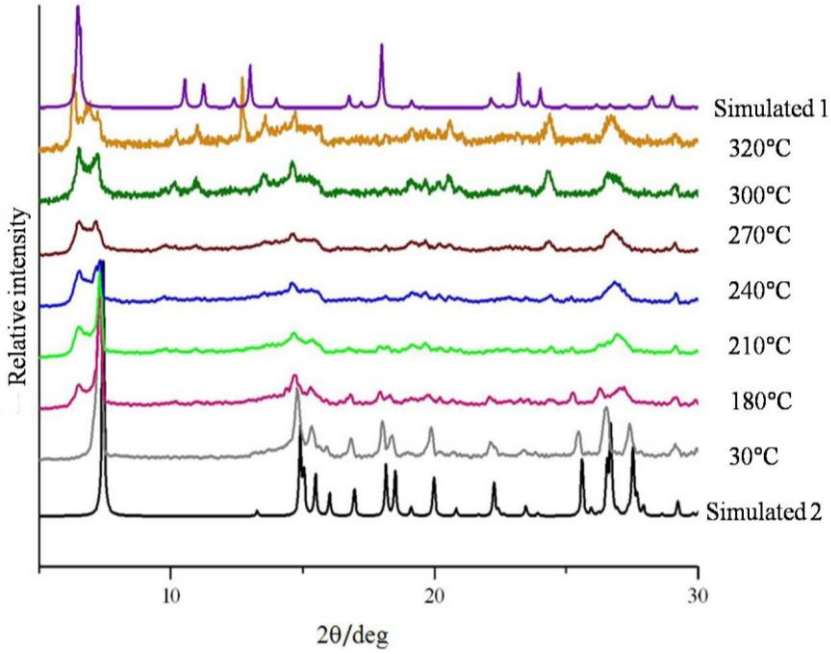

Figrue S5. T-PXRD pattern for **2**. Variable temperature PXRD was carried out from 30 °C to 320 °C according to the TGA and DSC analysis which revealed the dehydration temperature region. It could be seen that the transformation is not complete, but the crystalline sample maintained its crystallinity above until 320 °C to show partial transformation.

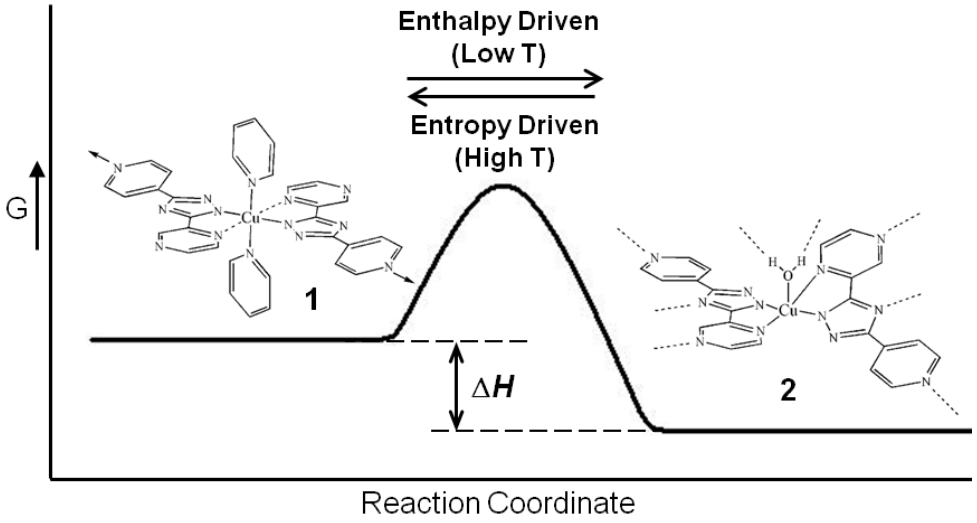

Scheme S2. Proposed reversible chemical equilibrium between **1** and **2** (arrow: coordination bonding; dashed line: weak bonding).

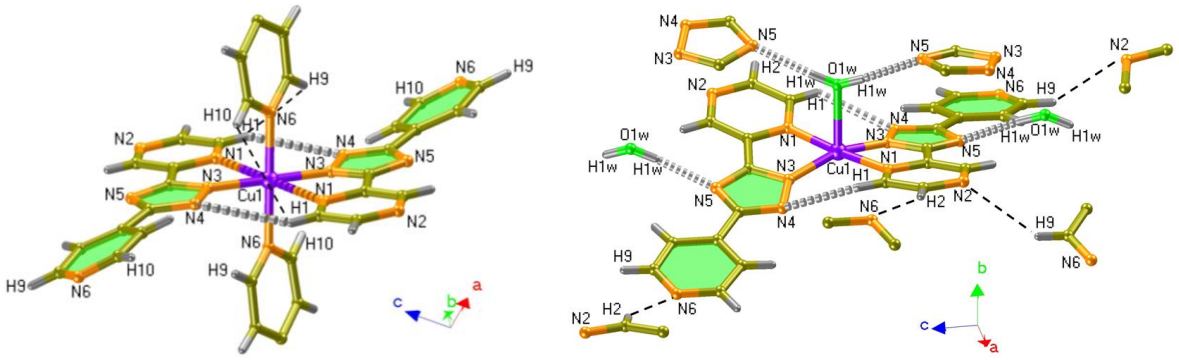

(a) (b)

Figure S6. Partial views of the labelled structures of **1** (a) and **2** (b), showing the deformable tectons and corresponding intra- and inter-molecular bonding details. In (a), gray dashed cones represent hydrogen bonding, and black dashed lines represent C–H···H–C contacts (other two pairs in the below pyridyl ring were omitted); in (b) gray dashed cones represent strong hydrogen bonding, and black dashed lines represent weak hydrogen bonding (other four pairs in the farther rings were omitted). The green planes highlight the distortion of the pyridyl rings in (a) and the deformation of the tecton in (b).